



# EXPERIMENTAL INVESTIGATIONS AND PARAMETER OPTIMIZATION OF LASER MACHINING PROCESS PARAMETERS USING NATURE BASED OPTIMIZATION TECHNIQUES

Sagar Hiwale, Rajiv Basavarajappa

College of Engineering Pune, Department of Manufacturing Engineering & Industrial Management, Pune- 411005, India

Corresponding author: Sagar Hiwale, hiwalesagar@gmail.com

**Abstract:** Laser machining is a thermal based process which is widely used to produce complex shapes geometry in difficult to hard materials. To produce complex profiles using traditional process is difficult task and time consuming. The optimum setting of laser process parameters is required to obtain desired accuracy in workpiece profile. To achieve this goal, an experimental investigation is attempted on CNC based Prima 4000W CW-CO<sub>2</sub> laser cutting process to machined material Hastelloy C- 276. The laser process parameters like, laser power, cutting speed, gas pressure, working distance and focal position are selected to obtain the influence on heat affected zone (HAZ) and average surface roughness (*Ra*) using response surface method (RSM). The significance of the process parameters are obtained for considered responses by performing ANOVA analysis. A regression model is developed for each response, i.e., HAZ and *Ra* to obtain the optimum setting of laser process parameters using black hole (BH) and krill herd (KH) algorithm. The considered algorithm mimics the nature phenomenon based on physics of stars and biological behaviour of krill creatures respectively. The result obtained using KH algorithm are found better compared to BH algorithm for the considered process. The confirmatory tests are performed for both the approaches, i.e., RSM and selected algorithm and it is observed that results are within percentage of error less than 5 %. The confirmatory test proves that the selected approaches are effective in obtaining the optimum parameters of considered process.

**Key words:** Laser machining process, response surface method, optimization, surface roughness, heat affected zone.

## 1. INTRODUCTION

In today's modern era, manufacturing industries produces complex geometry in difficult to hard materials in the desired product for which there is a necessity of advance processes. The advance process should be equipped with definite mechanism which can produce complex geometries in the workpiece materials. In this paper, a non – contact thermal based laser process is used for machining selected material Hastelloy C-276. The considered process is widely used by the industries due to its utmost significance

in obtaining desirable quality of profile cut. The laser machining process has different process parameters which has influence on the quality of cut. The desired quality of output characteristics can be obtained by the proper selection of these laser process parameters. In this paper, Hastelloy C-276 is machined using laser machining process to investigate the influence of laser process parameter for desired quality of cut.

In the literature, Caydus and Hascalik [1] have attempted parametric optimization using grey relational approach to obtain the optimum laser process parameters, i.e., cutting speed and power to enhance the performance characteristics, i.e., *Ra*, *kerf*, and HAZ. Salem et al. [2] have conducted experimental investigation to obtain the influence of laser process parameters i.e., scanning speed, power, and gas pressure on the performance characteristics hardness, and microstructure and oxide layer width for thin sheets of ultra-low carbon steel. The application of laser beam machining and future direction to enhance the capability of the considered process was reviewed in the literature by Dubey and Yadava [3] and Patidar and Rana [4]. Stournaras et al. [5] has performed a statistical analysis using experimental data to determine the contribution of laser process parameters in the influence of characteristics kerf width, *Ra* and HAZ during machining of aluminum 5083 alloy. Riveiro et al. [6] have attempted parametric investigation to demonstrate the influence of laser process parameters on edge surface aspect, dress characteristics and HAZ during machining of material aluminium 2024-T3. The result reveals that surface quality was improved at higher value of cutting speed and laser power.

Eltawahni et al. [7] have performed experimental investigation on CO<sub>2</sub> laser process to obtain the influence of laser process parameters on the performance characteristics kerf ratio, *Ra* and cost for different thickness of material MDF wood composite material using RSM approach. Zhian et al. [8] have proposed a graphical user interface for fuzzy expert system to predict the output characteristics *Ra* and

*dross inclusion* while machining of material Inconel 800 using laser machining process. Eltawahni et al. [9] have performed a statistical analysis using experimental data obtained using RSM approach to determine the influence of laser process parameters on characteristics, i.e., *kerf* characteristics ratio, *Ra* and operating cost during machining of AISI316 austenitic stainless steel. Scintilla and Tricarico [10] have developed a steady state simplified model to determine the average cutting temperature for performance measure of CO<sub>2</sub> based laser and solid state laser. They have performed numerical simulation to evaluate the conductive losses in laser machining process. Hashim et al. [11] have performed laser surface treatment under argon atmosphere condition to enhance wear resistance for the material Hastelloy C-276 and obtained optimum laser parameter setting that forms wear resistance surface without formation of brittle phase.

Hascalik and Ay [12] have investigated the effects of selected laser cutting process parameters to determine their influence on *Ra* and *HAZ* during machining of Inconel 718 nickel based super alloy. They have examined cutting defects, formed carbide surfaces and *kerf* size variation using instrument like, scanning electron microscope and X-ray diffraction. Manikandan et al. [13] have performed microstructure and macrostructure analysis for specimen joint made of material Hastelloy C 276 using gas tungsten arc welding and pulsed current gas tungsten arc welding. The result shows that the pulsed has produced improved weld strength, refined microstructure and reduced micro segregation. Adalarasan et al. [14] have performed experimental investigation on pulsed CO<sub>2</sub> laser process to obtain the influence of laser process parameters i.e., laser power, pulsing frequency, cutting speed and assist gas pressure on the performance characteristics *kerf* width, *Ra* and cut edge slope for Al6061/SiCp/Al<sub>2</sub>O<sub>3</sub> composite using grey based RSM. Ghavidel et al. [15] have investigated the effects of multi walled carbon nano tubes, laser power and feed rate on output characteristics *HAZ*, *kerf* width and *kerf* taper using full factorial based set of experiments. In other paper, Adalarasan et al. [16] have obtained the optimum value of laser process parameters on the performance characteristics *Ra* and *HAZ* for Al6061/Al<sub>2</sub>O<sub>3</sub> composite using Taguchi based RSM. Medic et al. [17] has attempted preference selection index method to obtain the optimum CO<sub>2</sub> laser cutting process parameters which enhance the desired characteristics, i.e., *Ra*, *HAZ*, *kerf* width and material removal rate (*MRR*) during machining of material stainless steel.

Moradi et al. [18] have performed a statistical analysis using experimental data based on RSM approach to determine the influence of laser process

parameters, i.e., laser power, cutting speed, focal position on characteristics "*Ra* and *geometry*" during machining of polycarbonate sheets. Zhang and Lei [19] has used an adaptive neural fuzzy inference system based neural network to predict the roughness using the experimental data and proposed that considered system overcomes the trap of local optimum solution. Rajaram et al. [20] has studied the significance of power and feed rate on *Ra*, *HAZ*, *kerf* width and *striation frequency* during machining of AISI4130 steel using CO<sub>2</sub> laser cutting. It was observed that power has substantial effect on *kerf* width and *HAZ* followed by feed rate. Gadallah and Abdu [21] have investigated the influence of cutting parameters like pressure, power, cutting speed, and frequency on *HAZ*, *Ra* and *kerf* taper during machining of stainless steel (316L) using experimental based approach.

The current literature focused on a comprehensive overview of the laser machining of selected materials and showed their advantages for fine machining, studied the surface characteristics, reviewed the development of laser process and effects of process parameter. However, studies on the laser cut quality of Hastelloy C276 are rather lacking. In this paper, an investigation is performed to obtain optimum setting for laser machining process parameters. A nickel based super alloy Hastelloy C276 is selected in the current study that has wide application in nuclear and chemical industries, pulp and paper production, municipal waste treatment, flue gas desulfurization etc. The analysis of the process parameters like, laser power, cutting speed, gas pressure, working distance and focal position is carried out to obtain the influence on performance characteristics *HAZ* and *Ra* using RSM based ANOVA. A set of approximate optimum parameter setting is obtained using selected nature based optimization techniques, i.e., black hole (BH) and krill herd (KH) algorithm. The considered algorithms are found effective to obtain effects of selected laser process parameter with respect to the considered performance characteristics, i.e., *HAZ* and *Ra*.

## 2. EXPERIMENT SETUP

In the present work, experiments are conducted on the CNC based prima 4000W CW CO<sub>2</sub> laser process as shown in Figure 1. The setup was used to conduct selected experiments which would analyze the effects of laser parameters like, laser power, cutting speed, gas pressure, working distance and focal position on required performance characteristics *Ra* and *HAZ*. The schematic diagram of geometrical features like, *Ra* and *HAZ* are shown in Figure 2. The workpiece material selected for carried out the experimentation is Hastelloy C276 having 3.7 mm thickness. The

chemical composition of considered workpiece material is 16.5 % Mo, 6.2 % Fe, 3.11 % W, 0.11 % V, 0.6 % Mn, 0.087 % Co, 0.034 % Si, 0.001 % S, 0.004 % P, 15.5 % Cr and balance Ni. A coaxial conical shaped laser nozzle having 2.5 mm diameter and focal length of lens as 190.5 (constant) is used to blow the gas mixture at constant flow rate on workpiece material.

The choice of the control factors to perform experiments is significant as they influence performance of the process. The selected parameters for the present work are laser power, cutting speed, gas pressure, working distance and focal position. The selected range of process parameters during the experimentation for laser power as 2400 (watt) to 3800 (watt), cutting speed as 1125 (mm/min) to 2400 (mm/min), gas pressure as 11 (bar) to 17 (bar), working distance as 0.5 (mm) to 1.50 (mm) and focus position as -4.20 (mm) to 0.5 (mm). The pilot experiments are used to determine the ranges and levels of control factors. The output characteristics *Ra* and *HAZ* are selected to analyze the influence of selected laser process parameters.



Fig. 1. Laser beam machine setup

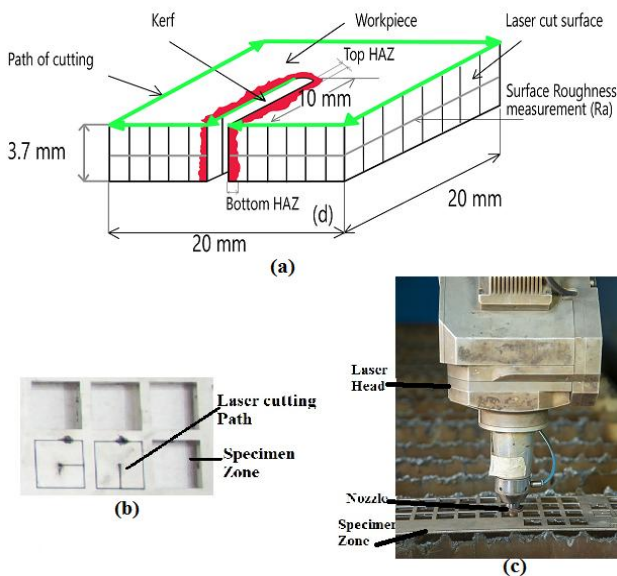


Fig. 2. Geometrical features the kerf characteristics (a) CAD model (b) Specimen and its cutting path (c) Laser head used for cutting specimen

Table 1. Experiment results using DOE

Sr	Laser power (watt)	Cutting speed (mm/min)	Gas pressure (bar)	Working Distance (mm)	Focus Position (mm)	<i>Ra</i> ( $\mu\text{m}$ )	<i>HAZ</i> (mm)
1	3394.31	1494.46	12.74	0.79	-2.84	1.25	0.213
2	3394.31	1494.46	15.26	1.21	-0.86	1.12	0.164
3	3394.31	2030.54	12.74	1.21	-2.84	1.07	0.232
4	3100.00	1762.50	14.00	1.00	0.50	0.97	0.173
5	3394.31	1494.46	15.26	0.79	-0.86	1.10	0.175
6	3100.00	1762.50	14.00	1.00	-4.20	0.92	0.233
7	2805.69	1494.46	12.74	1.21	-2.84	0.85	0.190
8	3394.31	1494.46	15.26	1.21	-2.84	1.10	0.216
9	3100.00	1762.50	14.00	1.00	-1.85	0.95	0.186
1	3100.00	1762.50	14.00	1.50	-1.85	0.90	0.187
1	3100.00	1762.50	14.00	1.00	-1.85	0.96	0.197
1	3100.00	1762.50	17.00	1.00	-1.85	0.96	0.149
1	2805.69	1494.46	12.74	1.21	-0.86	0.87	0.148
1	2805.69	2030.54	15.26	1.21	-0.86	1.04	0.207
1	2805.69	1494.46	15.26	1.21	-2.84	0.86	0.208
1	3100.00	1762.50	14.00	1.00	-1.85	0.97	0.193
1	2805.69	2030.54	12.74	0.79	-0.86	0.92	0.176
1	3394.31	1494.46	12.74	1.21	-0.86	1.13	0.184
1	2805.69	1494.46	15.26	1.21	-0.86	0.94	0.181
2	2805.69	2030.54	15.26	0.79	-0.86	0.88	0.158
2	3100.00	1762.50	14.00	1.00	-1.85	0.97	0.209
2	3394.31	2030.54	15.26	1.21	-2.84	1.00	0.217
2	3100.00	1125.00	14.00	1.00	-1.85	1.11	0.233
2	2805.69	1494.46	12.74	0.79	-0.86	0.94	0.198
2	3100.00	1762.50	14.00	0.50	-1.85	0.86	0.144
2	3394.31	1494.46	12.74	1.21	-2.84	1.16	0.212
2	2805.69	2030.54	12.74	1.21	-0.86	0.96	0.167
2	3394.31	1494.46	15.26	0.79	-2.84	1.07	0.168
2	3100.00	2400.00	14.00	1.00	-1.85	1.00	0.229
3	2400.00	1762.50	14.00	1.00	-1.85	0.84	0.155
3	3100.00	1762.50	14.00	1.00	-1.85	0.98	0.198
3	3394.31	2030.54	12.74	0.79	-0.86	0.99	0.198
3	3100.00	1762.50	14.00	1.00	-1.85	0.98	0.197
3	2805.69	1494.46	15.26	0.79	-0.86	0.89	0.178
3	3100.00	1762.50	14.00	1.00	-1.85	0.97	0.194
3	3100.00	1762.50	14.00	1.00	-1.85	0.98	0.212
3	3100.00	1762.50	14.00	1.00	-1.85	1.01	0.184
3	3394.31	1494.46	12.74	0.79	-0.86	1.23	0.203
3	3394.31	2030.54	12.74	0.79	-2.84	1.12	0.208
4	3394.31	2030.54	12.74	1.21	-0.86	1.08	0.242
4	2805.69	2030.54	12.74	1.21	-2.84	0.97	0.198
4	3394.31	2030.54	15.26	0.79	-0.86	0.94	0.149
4	3394.31	2030.54	15.26	0.79	-2.84	0.89	0.148
4	3800.00	1762.50	14.00	1.00	-1.85	1.17	0.180
4	2805.69	1494.46	15.26	0.79	-2.84	0.85	0.159
4	2805.69	2030.54	15.26	0.79	-2.84	0.85	0.178
4	3100.00	1762.50	11.00	1.00	-1.85	1.08	0.220
4	2805.69	2030.54	15.26	1.21	-2.84	0.90	0.203
4	2805.69	1494.46	12.74	0.79	-2.84	0.92	0.211
5	3394.31	2030.54	15.26	1.21	-0.86	1.06	0.221
5	3100.00	1762.50	14.00	1.00	-1.85	0.99	0.179
5	2805.69	2030.54	12.74	0.79	-2.84	0.92	0.179

The process parameter *Ra* is measured using Mitutoyo type surface test SJ 210 having a diamond conical stylus with a tip radius of  $4\mu\text{m}$  which is represented by a center line average (*Ra*) method. Measurements have been taken with the stylus

movement speed of 0.5 mm/s over an evaluation length of 2 cm per side of the cube. The specimen has size of 20 mm × 20 mm × 3.7mm as depicted in Figure 2(b). Average *Ra* is recorded at the end of the surface roughness measurement in the experimental data. During the experimentation, a 10 mm long straight cut is made on each specimen to determine the desired output characteristics. An equipment scanning electron microscope (Model: Sigma HV) was utilized to measure *HAZ*. Specimens are prepared using sandpaper with 60–600 mesh was used to grind the close surface texture. At the end of grinding process, the surfaces were cleaned and polished using diamond paste and solvent. The aquaregia solution consists of 5ml nitric acid (HNO<sub>3</sub>) and 15ml hydro chloric acid (HCl) was used to etch the polished specimens. The SEM is equipped with tungsten filament in high vacuum mode with variable accelerating voltage up to 30 KV, resolution range: 1.3 nm (20 KV) to 2.8 nm (1 KV) and magnification range: 50 X to 1000000 X. The layout of the experiment plan designed using rotatable central composite second order with experimental results obtained are shown in Table 1.

### 3. METHODOLOGY

Response surface method (RSM) is a statistical technique which is used for modeling and analysis of the given problem of interest governed by several variables and the objective is to optimize the performance output. RSM used sequential procedure to determine the optimum setting of the given problem by performing set of experiments which in turn used for building the regression models consist of independent and dependent variables. In the present work, the independent variables are laser power, cutting speed, gas pressure, working distance and focus position which are utilized to analyze the effect on performance characteristics *Ra* and *HAZ*. In compared to full factorial and Taguchi method, RSM reduces the number of experiments without compromising the goal of work, i.e., to obtain the optimum setting of process parameters. The general second order equation governed to obtain the values of models is given in equation (1)

$$y = \beta_0 + \sum_{i=1}^k \beta_i x_i + \sum_{i=1}^k \beta_{ii} x_{ii}^2 + \sum_i \sum_j \beta_{ij} x_i x_j + \varepsilon \quad (1)$$

where,

$y$  is the final response,  $x_i$  is the  $i^{th}$  process parameter,  $\beta_i$ ,  $\beta_{ij}$  are the general regression coefficients,  $\varepsilon$  is the error obtained in experiment,  $\beta_0$  constant.

By using a least square method, the values of the general regression coefficient can be obtained [22–23]. The capability of RSM is able to analyze the

effects of each process parameter and interactions parameters. In order to analyze the response characteristics like, *Ra* and *HAZ*, second order regression models is developed using the set of 52 experiments on the considered material. The final second order regression models in coded form obtained for the considered characteristics, i.e., *Ra* and *HAZ* are given in equations (2) and (3) using the experimental results given in Table 1.

$$\begin{aligned} Ra = & 0.97718 + 0.18220 x_1 - 0.05326 x_2 - 0.04590 x_3 + \\ & 0.03778 x_4 + 0.03401 x_5 + 0.0312 x_1^2 + 0.0812 x_2^2 + \\ & 0.0424 x_3^2 - 0.0938 x_4^2 - 0.0288 x_5^2 - 0.2350 x_1 x_2 - \\ & 0.0947 x_1 x_3 - 0.0159 x_1 x_4 - 0.0582 x_1 x_5 - 0.0078 x_2 x_3 + \\ & 0.1398 x_2 x_4 - 0.0018 x_2 x_5 + 0.1074 x_3 x_4 + \\ & 0.0854 x_3 x_5 + 0.0477 x_4 x_5 \end{aligned} \quad (2)$$

$$\begin{aligned} HAZ = & 0.198 + 0.019 x_1 + 0.006 x_2 + 0.028 x_3 + \\ & 0.032 x_4 + 0.018 x_5 + 0.035 x_1^2 + 0.024 x_2^2 + 0.012 x_3^2 + \\ & 0.037 x_4^2 + 0.003 x_5^2 + 0.036 x_1 x_2 + 0.013 x_1 x_3 + \\ & 0.005 x_1 x_4 + 0.001 x_1 x_5 + 0.017 x_2 x_3 + 0.054 x_2 x_4 + \\ & 0.014 x_2 x_5 + 0.052 x_3 x_4 + 0.005 x_3 x_5 + 0.018 x_4 x_5 \end{aligned} \quad (3)$$

where,

$x_1$  is laser power (watts),  $x_2$  is cutting speed (mm/min),  $x_3$  is gas pressure (bar),  $x_4$  is working distance (mm) and  $x_5$  is focal position (mm).

In the subsequent section, the analysis of variance (ANOVA) analysis to check the adequacy of the developed regression models for *Ra* and *HAZ* is reported. The detailed result and discussion for the influence of process parameters are given as under.

#### 3.1 Analysis of Ra

The ANOVA results for the obtained quadratic model of *Ra* are shown in Table 2. It is found from Table 2 that the model is significant as the obtained F-value is 56.01. It is found that the model terms along with square terms of laser power ( $x_1$ ), working distance ( $x_4$ ) and interaction terms i.e.,  $x_1 x_2$ ,  $x_1 x_3$ ,  $x_2 x_4$  are significant as the value of Prob > F is less than 0.05. The corresponding F-value of each term i.e., linear, squared and interaction are reported in Table 2, the term with higher F-value would have the more significance, i.e., here the F-value of laser power. It is observed that the F-value of laser power is 514.68 which are higher compared to other parameters. It reveals from Table 2 that the parameter laser power has higher effects on *Ra* followed by other considered parameters. With reference to F-value, the parameter focus position with F-value as 17.97 has least effect on *Ra*. The obtained value of Pred R-Squared as 0.9098 shows good agreement with the value of Adj R-Squared as 0.9557 i.e. the difference found to be less than 0.2.

The influence of selected laser machining parameters like laser power ( $x_1$ ), cutting speed ( $x_2$ ), gas pressure ( $x_3$ ) working distance ( $x_4$ ), focus position ( $x_5$ ) on *Ra* is

shown in Figure 3 (a) and (b). As the value of laser power increases the performance characteristic  $R_a$  is degraded gradually (Figure 3 (a)). This occurs due to the fact that as the value of laser power increases, its intensity on the workpiece material for machining increases which degrades the side face of the specimen as shown in Figure 3(a) and (b).

Table 2. ANOVA analysis of  $R_a$

Source	Sum of Squares	Degree of freedom	Mean Square	F Value	p-value Prob>F
Model	20	0.512778	0.02563	56.01	<0.001
Linear	5	0.289386	0.05787	126.43	<0.001
Laser power ( $x_1$ )	1	0.235606	0.23560	514.68	<0.001
Cutting speed ( $x_2$ )	1	0.020109	0.02010	43.93	0.041
Gas pressure ( $x_3$ )	1	0.015298	0.01529	33.42	0.064
Working distance ( $x_4$ )	1	0.010108	0.01010	22.08	0.120
Focus position ( $x_5$ )	1	0.008227	0.00822	17.97	0.163
$x_1^2$	1	0.001785	0.00178	3.90	0.057
$x_2^2$	1	0.012109	0.01210	26.45	<0.001
$x_3^2$	1	0.003904	0.00390	8.53	0.006
$x_4^2$	1	0.016133	0.01613	35.24	<0.001
$x_5^2$	1	0.001521	0.00152	3.32	0.078
$x_1 x_2$	1	0.055279	0.05527	120.76	<0.001
$x_1 x_3$	1	0.013075	0.01307	28.56	<0.001
$x_1 x_4$	1	0.000254	0.00025	0.55	0.462
$x_1 x_5$	1	0.003405	0.00340	7.44	0.010
$x_2 x_3$	1	0.000090	0.00009	0.20	0.661
$x_2 x_4$	1	0.019503	0.01950	42.60	<0.001
$x_2 x_5$	1	0.000003	0.00000	0.01	0.935
$x_3 x_4$	1	0.016761	0.01676	36.61	0.017
$x_3 x_5$	1	0.010658	0.01065	23.28	0.217
$x_4 x_5$	1	0.002278	0.00227	4.98	0.033
Error	31	0.014191	0.01419		
Lack-of-Fit	22	0.011751	0.01175	1.97	0.147
Pure Error	9	0.002440	0.00244		
Total	51	0.526969			
S: 0.0213955, R <sup>2</sup> :97.31 %				R <sup>2</sup> (predicted): 90.98%	
R <sup>2</sup> (adjacent): 95.57%					

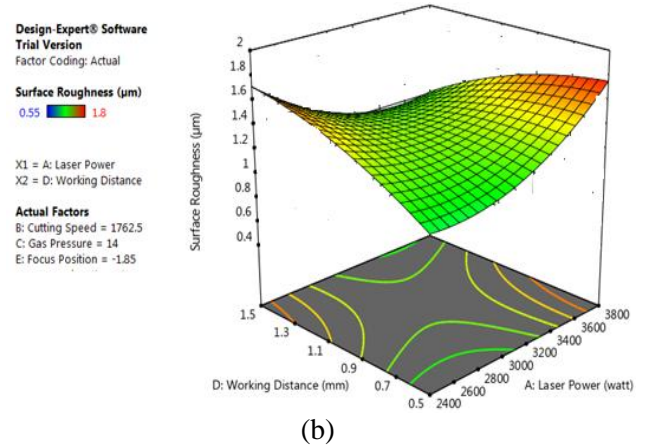


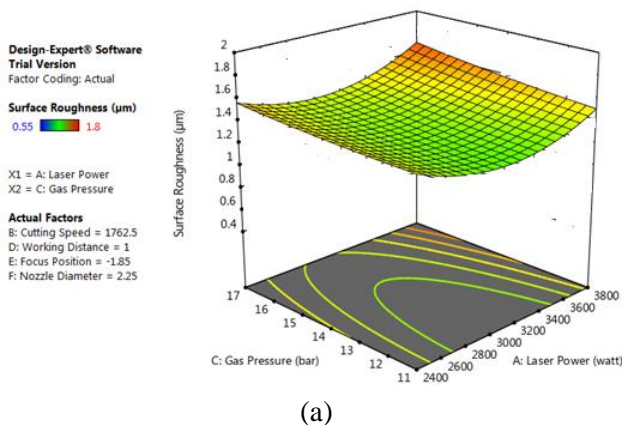
Fig. 3. Response surface plots of  $R_a$  for significant process parameters: (a) laser power and gas pressure, (b) working distance and laser power

To reduce the effect laser power on  $R_a$  minimum value is desirable. It is observed from Figure 3 (a) as the value of gas pressure increases, the performance characteristics  $R_a$  improved. This is due to the fact that as the value of gas pressure increases it creates thrust at side face along with laser power which produces intense energy to cut the specimen smoothly.

As the value of working distance increases, the value of  $R_a$  degrades. This is due the fact that when the working distance i.e., distance between nozzle and specimen increased, the energy transfer rate will be reduced which creates difficulty in machining of the specimen result in degrade value of  $R_a$ . The effects of working distance on  $R_a$  with respect to laser power are shown in Figure 3 (b). The focus position has least effect on the parameter  $R_a$  as F-value obtained is very less compared to other parameters as depicted in Table 2.

### 3.2 Analysis of HAZ

The ANOVA results for the obtained quadratic model of HAZ are shown in Table 3. It is found from Table 3 that the model is found to be significant as the obtained F-value is 55.9. From Table 3, it is found that the model terms along with square terms of laser power ( $x_1$ ), gas pressure ( $x_3$ ), working distance ( $x_4$ ) and interaction terms i.e.,  $x_1 x_2$ ,  $x_1 x_3$ ,  $x_2 x_3$ ,  $x_2 x_4$ ,  $x_3 x_4$ ,  $x_4 x_5$  are significant as the value of Prob>F is less than 0.05. The corresponding F-value of each term i.e., linear, squared and interaction are reported in Table 3, the term with higher F-value would have the more significance. From Table 3, it is observed that the F-value of working distance is 256.7 which are higher compared to other parameters. It reveals from Table 3 that the parameter working distance and gas pressure has higher effects on HAZ followed by parameter laser power. With reference to F-value, the parameter cutting speed with F-



value as 7.5 has least effect on *HAZ*. The obtained value of Pred R-Squared as 0.9085 shows good agreement with the value of Adj R-Squared as 0.9556 i.e. the difference found to be less than 0.2. The influence of laser machining process parameters like laser power ( $x_1$ ), cutting speed ( $x_2$ ), gas pressure ( $x_3$ ) working distance ( $x_4$ ), focus position ( $x_5$ ) on *HAZ* is shown in Figure 4 (a) –(c). During the laser machining of material Hastelloy C-276 an unavoidable occurrence of *HAZ* can be observed from Figure 5. As the value of laser power increases the performance characteristic *HAZ* is increased gradually (Figure 4 (a)). This happens due to the fact that as the value of laser power increases, its intensity on the workpiece material for machining increases which degrades the side upper face of cutting zone as shown in Figure 5. To reduce the effect laser power on *HAZ* minimum value is desirable. It is observed from Figure 4 (a) as the value of cutting speed increases, the performance characteristics *HAZ* decreases. As the value of cutting speed increases, it reduces the time for machining and interaction of laser power with the workpiece material results in desirable *HAZ*.

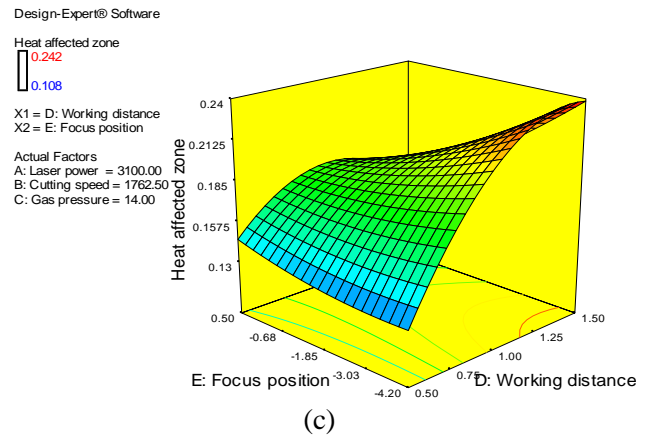
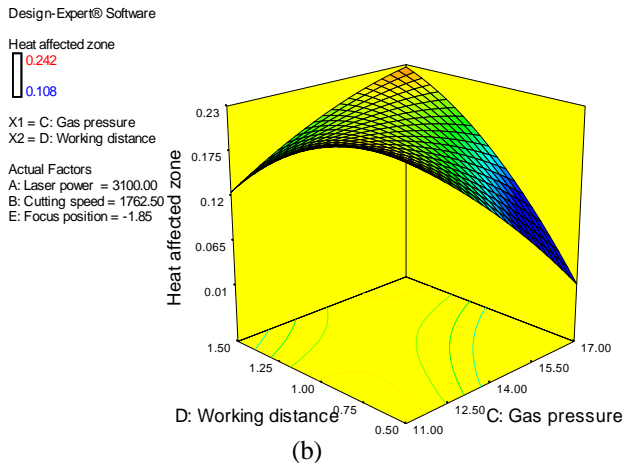
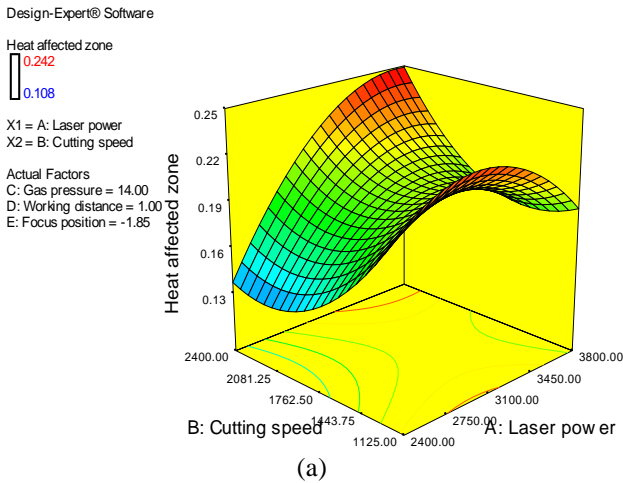


Fig. 4. Response surface plots of *HAZ* for significant process parameters (a) laser power and cutting speed, (b) working distance and gas pressure, (c) working distance and focus position

It is revealed from the Figure 4 (a) that the minimum *HAZ* is achieved at 2400 watts laser power, 2400 mm/min cutting speed, 14 bar gas pressure, 1 mm working distance and 1.85 mm focus position. The effects of laser power on *HAZ* with respect to cutting speed are shown in Figure 4 (a).

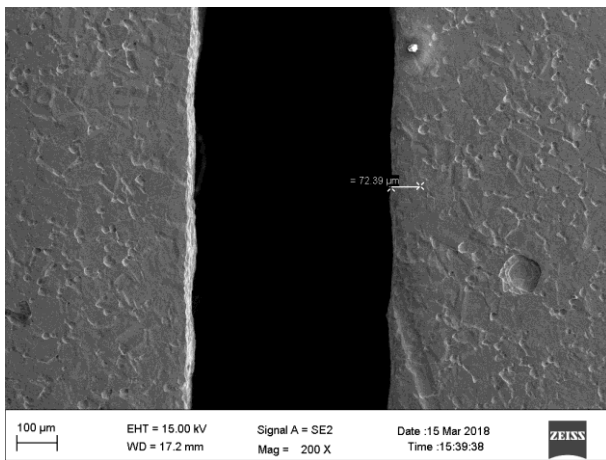
It is observed from the Figure 4 (b) as the gas pressure and working distance increases; there is a gradual decrease in the performance characteristics *HAZ*. Whenever the value of gas pressure and working distance increases simultaneously, the focused of the beam is more confine towards the cut results in reduction of *HAZ*. Further, gas pressure contributes to the cooling of the workpiece and thus, higher values of gas pressure contribute towards reduction in the amount of the surrounding *HAZ*.

It is concluded that the minimum *HAZ* would occurs at lower values of laser power and higher value of working distance, cutting speed and focus position. The effects of working distance on *HAZ* with respect to focus position are shown in Figure 4 (c). It is observed form Figure 4(c) that focus position has little effect compared to the working distance which has strong influence on the parameter *HAZ*.

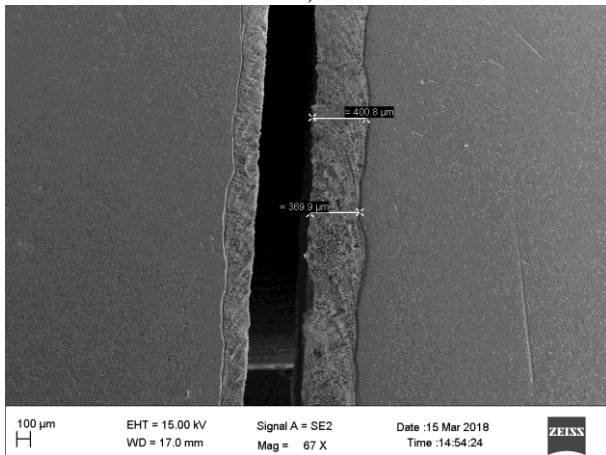
Table 3. ANOVA analysis of *HAZ*

Source	Sum of Squares	Degree of freedom	Mean Square	F Value	p-value Prob> F
Model	20	0.031847	0.001592	55.9	< 0.001
Linear	5	0.017987	0.003597	126.3	< 0.001
Laser power ( $x_1$ )	1	0.002617	0.002617	91.9	< 0.001
Cutting speed ( $x_2$ )	1	0.000214	0.000214	7.5	0.010
Gas pressure ( $x_3$ )	1	0.005540	0.005540	194.4	< 0.001
Working distance ( $x_4$ )	1	0.007315	0.007315	256.7	< 0.001
Focus position ( $x_5$ )	1	0.002298	0.002298	80.7	< 0.001
$x_1^2$	1	0.002193	0.002193	77.0	< 0.001
$x_2^2$	1	0.001083	0.001083	38.0	< 0.001
$x_3^2$	1	0.000337	0.000337	11.8	0.002

$x_4^2$	1	0.002545	0.002545	89.3	<0.001
$x_5^2$	1	0.000016	0.000016	0.6	0.465
$x_1 x_2$	1	0.001280	0.001280	44.9	<0.001
$x_1 x_3$	1	0.000234	0.000234	8.2	0.007
$x_1 x_4$	1	0.000024	0.000024	0.9	0.362
$x_1 x_5$	1	0.000001	0.000001	0.0	0.845
$x_2 x_3$	1	0.000437	0.000437	15.3	<0.001
$x_2 x_4$	1	0.002861	0.002861	100.4	<0.001
$x_2 x_5$	1	0.000189	0.000189	6.6	0.015
$x_3 x_4$	1	0.003862	0.003862	135.5	<0.001
$x_3 x_5$	1	0.000041	0.000041	1.5	0.238
$x_4 x_5$	1	0.000309	0.000309	10.8	0.002
Error	31	0.000883	0.000028		
Lack-of-Fit	22	0.000749	0.000034	2.3	0.102
Pure Error	9	0.000135	0.000015		
Total	51	0.032730			
S: 0.0053, R <sup>2</sup> : 97.30%		R <sup>2</sup> (adjacent): 95.56%		R <sup>2</sup> (predicted): 90.85%	



a)



b)

Fig. 5. Effect of laser process parameter on *HAZ* (a) Specimen: 1 ( $x_1$ : 2400 watts,  $x_2$ : 1200 mm/min,  $x_3$ : 13 bar,  $x_4$ : 1.5 mm,  $x_5$ : -1.5 mm) (b) Specimen: 2 ( $x_1$ : 3100 watts,  $x_2$ : 1762.5 mm/min,  $x_3$ : 11 bar,  $x_4$ : 1 mm,  $x_5$ : -1.85 mm)

### 3.3 Desirability analysis and confirmatory test

In this section, desirability analysis is carried out using RSM for the considered material Hastelloy C-276. The response *Ra* and *HAZ* is considered individually during the desirability analysis. A minimum level is set for considered output

characteristics *Ra* and *HAZ* which is required to be optimized. During the analysis the selected laser process parameters are kept under range bounds. The obtained optimum setting of process parameters for *laser power* as 2800.69 watts, *cutting speed* as 1494.46 mm/min, *gas pressure* as 15.26 bar, *working distance* as 0.79 mm and *focus position* as -2.84 mm for the response *Ra* as 0.85 mm with the desirability value as 1. As the obtained value of desirability is 1, it signifies the significance and improvement of the response *Ra*. While the obtained optimum process parameters are *laser power* as 3100 watts, *cutting speed* as 1762.5 mm/min, *gas pressure* as 14 bar, *working distance* as 0.5 mm and *focus position* as -1.85 mm for the response *HAZ* as 0.144 degree with the desirability value as 1. The optimal conditions are obtained using desirability analysis approach for the considered characteristics. However, it is necessary to confirm the results using confirmatory tests experiments. The confirmatory values are depicted in Table 4. The experimental confirmatory values obtained for the considered performance parameters *Ra* and *HAZ* as 0.91 and 0.150 respectively. The corresponding value of error obtained as 0.60 and 0.041 respectively.

Table 4. Confirmatory test result for desirability analysis

Response	$x_1$	$x_2$	$x_3$	$x_4$	$x_5$	Value*	Confir <sup>#</sup>	Error
<i>Ra</i>	2805.69	2030.54	15.26	0.79	-2.8	0.85	0.910	0.60
<i>HAZ</i>	3100	1762.5	14	0.5	-1.8	0.144	0.150	0.041

\*RSM obtained value, # Confirmatory test value

## 4. OPTIMIZATION TECHNIQUES

In this section, two nature based optimization techniques are applied to the regression models obtained using the experimental results for the workpiece material Hastelloy C-276. The reason to use these techniques is their effectiveness that is observed through the literature survey which proves its capability to solve the problems effectively.

### 4.1 Blackhole algorithm

Black hole concept is defined when a star having enormous mass is collapsed in space. It has a strong gravitational pull that the tiniest particle or light cannot escape from it. Based on this phenomenon, BH algorithm is introduced by Hatamlou [24]. It is a population-based algorithm and effectively implemented on various complex optimization problems. In BH algorithm, initial population of candidate solutions is called as stars and generated using random numbers. The candidate solution with maximum fitness is termed as black hole and other solutions are considered as normal stars. After initialization, black hole pulls the stars present around it and absorbs the star which comes very close to it

and gets disappeared permanently. A new search is started by randomly generating a new candidate or star and placed in the search space. A new population is developed by moving the candidate solutions towards the black hole i.e. best star which decides by the existing position and random number and substitutes those stars within the range of the black hole. The advantage of BH algorithm is that, it has less number of tuning parameters and operators to modify as compared to other algorithms. Eq. (4) is formulated to show the absorption of stars by the black hole:

$$x_i(t + 1) = x_i(t) + rand \times (x_{BH} - x_i(t)) \quad i = 1, 2, \dots, N(4)$$

where,

$x_i(t)$  and  $x_i(t + 1)$  are the positions of the  $i^{th}$  star at iterations  $t$  and  $(t + 1)$  respectively,  $x_{BH}$  is the position of the black hole in the search space,  $rand$  is a random number generated between  $[0, 1]$ ,  $N$  is the number of stars i.e. candidate solutions.

A schematic flowchart of BH algorithm is shown in Figure 6. The main steps of the BH algorithm steps are here in under [24]:

**Step 1.** Randomly generate the population of stars in search space.

**Step 2.** Calculate the objective for each star.

**Step 3.** Best star or solution is selected as black hole and other considered as normal stars.

**Step 4.** Change the position of stars by moving them towards black hole.

**Step 5.** The star with optimum value exchanges the position with the black hole.

**Step 6.** If a star goes beyond the limit of the black hole, then it is replaced with a new star.

**Step 7.** Repeat steps 3 to 7 until termination criterion is reached.

#### 4.2 Krill herd algorithm

KH algorithm is developed and tested by Gandomi and Alavi [25]. In this algorithm, the important elements are krill density and the distance between krill herd and food location. The krill positions are updated using three effective factors i.e. movement induced by other krill individuals, foraging activity and random diffusion. It mimics the behaviour of density krill and their position that are present in the deep sea.

The algorithm is quite feasible to obtain solutions of complex optimization problems. A Lagrangian model is given for KH algorithm as given in equation (5):

$$\frac{dx_i}{dx} = N_i + F_i + D_i \quad (5)$$

where,

$N_i$  is the motion induced by each krill,  $F_i$  is foraging motion and  $D_i$  is the diffusion parameter.

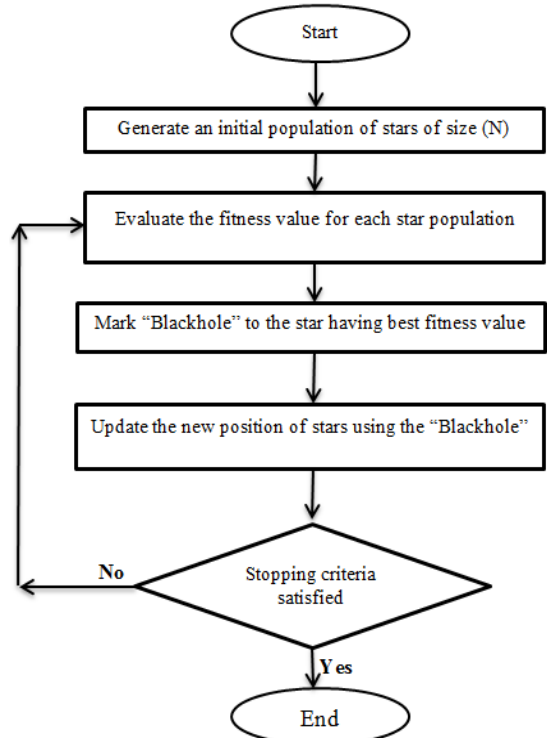


Fig. 6. Flowchart for BH algorithm

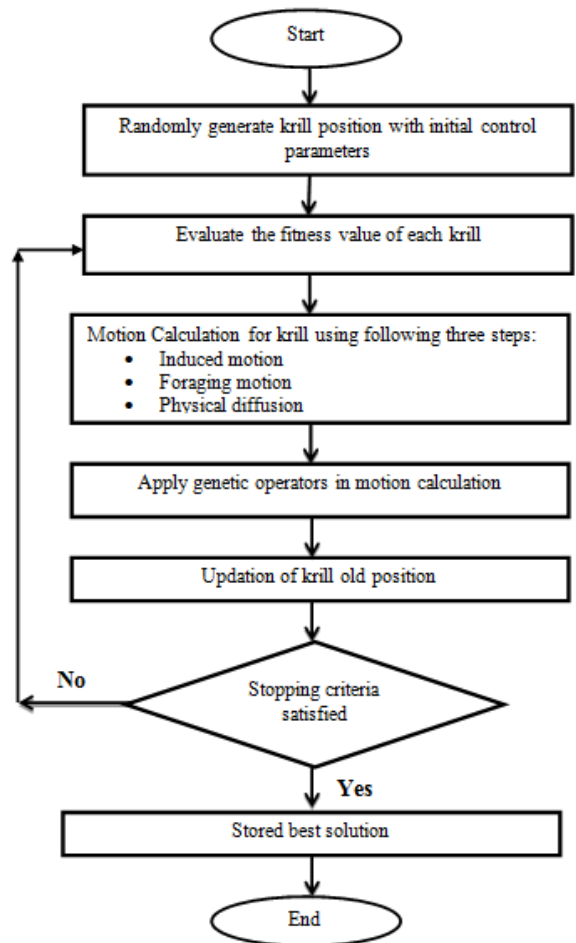


Fig. 7. Flowchart for KH algorithm

A schematic flowchart of KH algorithm is shown in Figure 7. The main steps of the KH algorithm steps are here in under [25].

**Step 1.** Krill individuals are generated using random population. Set the values for control parameters such as foraging speed, maximum diffusion speed and maximum induced speed.

**Step 2.** Based on the position of krill, evaluate the objective function value.

**Step 3.** Calculate the motion of each krill i.e. motion induced by other krill individuals, foraging motion and physical diffusion.

**Step 4.** Crossover and mutation operators are implemented.

**Step 5.** Update the positions of krill individual to obtain new population.

**Step 6.** Evaluate the objective function value of new krill individuals.

**Step 7.** Stop the algorithm, if termination criterion is reached else go to step 3.

#### 4.3 Results of single objective optimization

In the present study, the considered algorithm BH and KH are applied on equations (2) and (3) to measure the effectiveness. The performance characteristics, i.e.,  $Ra$  and  $HAZ$  are considered individually to optimize them separately, i.e., to minimize both the objective function. The convergence trend for  $Ra$  and  $HAZ$  obtained are shown in Figure 8 (a) and (b) respectively. The optimum result obtained using BH and KH algorithm are given in Table 5. When the result obtained using desirability analysis is compared with the results of BH and KH algorithm, it is observed that the results are quite similar to each other. The optimum result obtained using KH algorithm is found better compared to BH and RSM approach. In the response  $Ra$ , it is observed that the response value ( $Ra$ ) obtained using KH algorithm ( $0.3390 \mu\text{m}$ ) are far better compare to BH ( $0.6007 \mu\text{m}$ ) and RSM approach ( $0.85 \mu\text{m}$ ) as given in Table 5. Similarly, it is observed that the response value ( $HAZ$ ) obtained using KH algorithm ( $0.1410 \text{ mm}$ ) is found better compare to BH ( $0.1567 \text{ mm}$ ) and RSM approach ( $0.144 \text{ mm}$ ) as given in Table 5. Furthermore, the optimum solutions obtained for response  $Ra$  and  $HAZ$  using KH has higher success rate compared to BH algorithm. As seen from the Figure 8 (a) and (b), KH algorithm is converging faster compared to BH algorithm with 200 iterations and number of trials as 10. The optimum results shown in Table 5 are rounded off as given Table 6, so that they can be tuned on the considered process.

The mean, standard deviation and computational time obtained at the end of ten trials for the convergence of  $Ra$  and  $HAZ$  using BH algorithm are  $\{0.615, 0.161\}$ ,  $\{0.0293, 0.0041\}$  and  $\{0.213, 0.257\}$  respectively. while, the mean, standard deviation and computational time obtained at the end ten trials for the convergence of  $Ra$  and  $HAZ$  using KH algorithm are  $\{0.3981, 0.147\}$ ,  $\{0.077, 0.0017\}$  and  $\{9.85,$

$10.27\}$  respectively. On comparing the values of mean and standard deviation for the considered algorithms, the values obtained using KH algorithm is better than the BH algorithm.

The confirmatory test are performed to validate the result obtained using the considered algorithm. For this purpose, the values of process parameters are rounded off are used to perform confirmatory test experiments as given in Table 7.

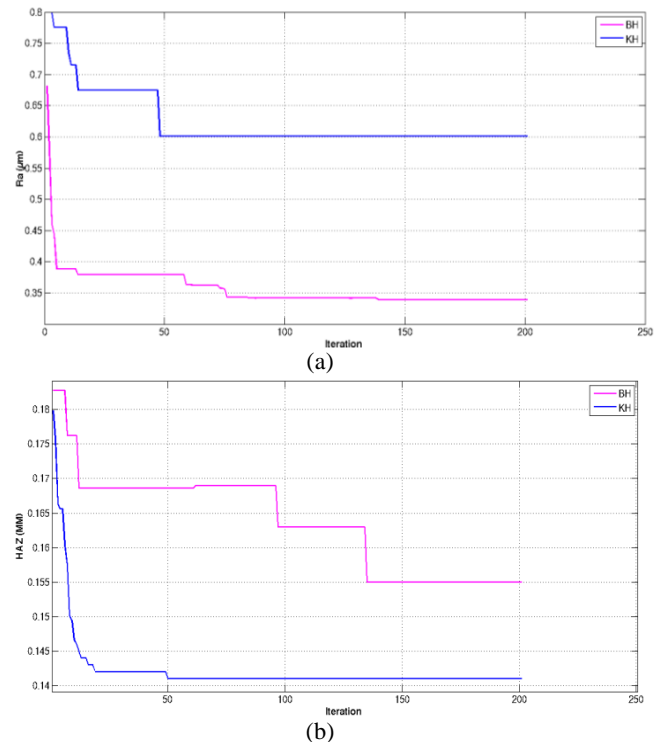


Fig. 8. Convergence of performance parameters using BH and KH algorithm (a)  $Ra$  (b)  $HAZ$

It is observed from the confirmatory test that difference between results of optimum values of process parameters using considered algorithm and test results shows the percentage error is within 6%. The rounded off values can be easily tuned on considered machining process to obtain desired output, i.e.,  $Ra$  and  $HAZ$  for the considered material.

#### 5. CONCLUSIONS

In this paper, the selected optimization techniques and RSM method are successfully applied to obtain the optimum laser machining process parameters for considered material Hastelloy C-276. The significance of laser process parameters on the considered characteristics  $Ra$  and  $HAZ$  are reported. It is observed that laser power has most influence on  $Ra$  with percentage contribution 44.71%. Similarly, working distance has most influence on  $HAZ$  with percentage contribution 22.3%. The optimum values obtained using desirability based RSM approach for  $Ra$  and  $HAZ$  are found as  $0.855 \mu\text{m}$  and  $0.144 \text{ mm}$  respectively. The considered BH and KH algorithm are applied to the

developed regression models of  $Ra$  and  $HAZ$ . These models of  $Ra$  and  $HAZ$  are optimized using considered algorithm to obtain the optimum setting of parameters. In the response  $Ra$ , it is found that the response value ( $Ra$ ) obtained using KH algorithm (0.3390  $\mu\text{m}$ ) is better compare to BH (0.6007  $\mu\text{m}$ ). Similarly, it is observed

that the response value ( $HAZ$ ) obtained using KH algorithm (0.1410 mm) is found better compare to BH (0.1567 mm). The results obtained using considered algorithm is confirmed using confirmatory test and it found that the percentage error is within 6%.

Table 5. Optimum results obtained using BH and KH algorithm

Algorithm	Response	Response value	Laser power (watt)		Cutting speed (mm/min)		Gas pressure (bar)		Working Distance (mm)		Focus Position (mm)	
			Coded	Actual	Coded	Actual	Coded	Actual	Coded	Actual	Coded	Actual
BHA	Ra ( $\mu\text{m}$ )	0.6007	-0.9609	2427.367	-0.3976	1508.979	-0.0547	13.8358	0.8024	1.4012	-0.7222	-3.547
	HAZ (mm)	0.1567	-0.8818	2482.760	0.8418	2299.17	0.4510	15.3532	-0.8486	0.5757	-0.5729	-3.1963
KHA	Ra ( $\mu\text{m}$ )	0.3390	-1	2400	-1	1125	-1	11	1	1.5	-1	-4.2
	HAZ (mm)	0.1410	-0.8791	2484.662	1	2400.00	0.9737	16.9211	-1	0.5000	-1	-4.2000

Table 6. Feasible (Rounded-off) optimum results obtained using BH and KH algorithm

Algorithm	Response	Response value	Laser power (watt)		Cutting speed (mm/min)		Gas pressure (bar)		Working Distance (mm)		Focus Position (mm)	
			Coded	Actual	Coded	Actual	Coded	Actual	Coded	Actual	Coded	Actual
BHA	Ra ( $\mu\text{m}$ )	0.6107	-0.9614	2427	-0.3976	1508	-0.0666	13.8	0.8000	1.4	-0.7021	-3.5
	HAZ (mm)	0.1569	-0.8814	2483	0.8416	2299	0.4666	15.4	-0.8400	0.58	-0.5745	-3.20
KHA	Ra ( $\mu\text{m}$ )	0.3390	-1	2400	-1	1125	-1	11	1	1.5	-1	-4.2
	HAZ (mm)	0.1405	-0.8786	2485	1	2400	0.9666	16.9	-1	0.5	-1	-4.2

Table 7. Confirmatory test results for results obtained using BH and KH algorithm

Algorithm	Response	Laser power (watt)	Cutting speed (mm/min)	Gas pressure (bar)	Working Distance (mm)	Focus Position (mm)	Response value	Confirmatory test result
BH	Ra ( $\mu\text{m}$ )	2427	1508	13.8	1.4	-3.5	0.6107	0.6831
	HAZ (mm)	2483	2299	15.4	0.58	-3.20	0.1569	0.1690
KH	Ra ( $\mu\text{m}$ )	2400	1125	11	1.5	-4.2	0.3390	0.3976
	HAZ (mm)	2485	2400	16.9	0.5	-4.2	0.1405	0.1521

## 6. REFERENCES

- Caydus, U. and Hascalik, A. (2008). *Use of the grey relational analysis to determine optimum laser cutting parameters with multi-performance characteristics*. Opt. Laser Technol. **40**, 987–994.
- Salem, H.G., Mansour, M.S., Badr, Y. and Abbas, W.A. (2008). *CW Nd: YAG laser cutting of ultra low carbon steel thin sheets using O<sub>2</sub> assist gas*. J. Mater. Process. Technol. **196**, 64–72.
- Dubey, A. K. and Yadava, V. (2008). *Laser beam machining — A review*. Int. J. Mach. Tools Manuf. **48**, 609–628.
- Patidar, D. and Rana, R. S. (2018). *The effect of CO<sub>2</sub> laser cutting parameter on mechanical and microstructural characteristics of high strength steel-A review*. Mater. Today Proc. **5**, 17753–17762.
- Stournaras, A., Stavropoulos, P., Salonitis, K. and Chryssolouris, G. (2009). *An investigation of quality in CO<sub>2</sub> laser cutting of aluminum*. CIRP J. Manuf. Sci. Technol. **2**, 61–69.
- Riveiro, A., Quintero, F., Lusqui, F. and Comesa, R. (2010). *Parametric investigation of CO<sub>2</sub> laser cutting of 2024-T3 alloy*. J. Mater. Process. Technol. **210**, 1138–1152.
- Eltawahni, H. A., Olabi, A. G. and Benyounis, K. Y. (2011). *Investigating the CO<sub>2</sub> laser cutting parameters of MDF wood composite material*. Opt. Laser Technol. **43**, 648–665.
- Zhian, C., Mokhtar, M., Jeng, C. and Manurung, Y. H. P. (2011). *Approach to prediction of laser cutting quality by employing fuzzy expert system*. Exp. Sys. Appl. **38**, 7558–7568.
- Eltawahni, H. A., Hagino, M., Benyounis, K. Y., Inoue, T. and Olabi, A. G. (2012). *Effect of CO<sub>2</sub> laser cutting process parameters on edge quality and operating cost of AISI316L*. Opt. Laser Technol. **44**, 1068–1082.
- Scintilla, L. D. and Tricarico, L. (2012). *Estimating cutting front temperature difference in disk and CO<sub>2</sub> laser beam fusion cutting*. Opt. Laser Technol. **44**, 1468–1479.
- Hashim, M., Raghavendra, K. E. S., Duraiselvam, M. and Natu, H. (2013). *Improvement of wear resistance of Hastelloy C-276 through laser surface melting*. Mater. Des. **46**, 546–551.
- Hascalik, A. and Ay, M. (2013). *CO<sub>2</sub> laser cut quality of Inconel 718 nickel – based superalloy*. Opt. Laser Technol. **48**, 554–564.

13. Manikandan, M., Arivazhagan, N., Rao, M. N. and Reddy, G. M. (2014). *Microstructure and mechanical properties of alloy C-276 weldments fabricated by continuous and pulsed current gas tungsten arc welding techniques*. J. Manuf. Process. **16**, 563–572.
14. Adalarasan, R., Santhanakumar, M. and Rajmohan, M. (2015). *Optimization of laser cutting parameters for Al6061 / SiCp / Al<sub>2</sub>O<sub>3</sub> composite using grey based response surface methodology*. Measurement, **73**, 596–606.
15. Ghavidel, A.K., Azdast, T., Reza, M. and Navidfar, A. (2015). *Effect of carbon nanotubes on laser cutting of multi-walled carbon nanotubes / poly methyl methacrylate nano composites*. Opt. Laser Technol. **67**, 119–124.
16. Adalarasan, R., Santhanakumar, M. and Thileepan, S. (2016). *Selection of optimal machining parameters in pulsed CO<sub>2</sub> laser cutting of Al6061/ Al<sub>2</sub>O<sub>3</sub> composite using Taguchi-based response surface methodology (T-RSM)*. Int. J. Adv. Manuf. Technol. doi:10.1007/s00170-016-8978-5
17. Madic, M., Antuchevicieneb, J., Radovanovica, M., Petkovic, D. (2017). *Determination of laser cutting process conditions using the preference selection index method*. Opt. Laser Technol. **89**, 214–220.
18. Moradi, M., Mehrabi, O., Azdast, T. and Benyounis, K. Y. (2017). *Enhancement of low power CO<sub>2</sub> laser cutting process for injection molded polycarbonate*. Opt. Laser Technol. **96**, 208–218.
19. Zhang, Y. and Lei, J. (2017). *Prediction of Laser cutting roughness in intelligent manufacturing mode based on ANFIS*. Procedia Eng. **174**, 82–89.
20. Rajaram, N., Sheikh-Ahmad, J. and Cheraghi, S.H. (2003). *CO<sub>2</sub> laser cut quality of 4130 steel*. Int. J. Mach. Tools Manuf. **43**, 351-358.
21. Gadallah, M.H. and Abdu, H.M. (2015). *Modeling and optimization of laser cutting operations*. Manuf. Review. **2**, 1- 15.
22. Paneerselvam, R. (2012). *Design and analysis of experiment*, PHI Learning Publisher, India.
23. Montgomery, D.C. (2010). *Design and analysis of experiments*, John Wiley and Sons publisher, NJ, USA.
24. Hatamlou, A. (2013). *Black hole: A new heuristic optimization approach for data clustering*. Inf. Sci. **222**, 175–184
25. Gandomi, A. H. and Alavi, A.H. (2012). *Krill herd: A new bio-inspired optimization algorithm*. Comm. Nonlinear Sci. Numer. Simul. **17**(12) 4831–4845.